Magnetic Resonance Image–Guided Transcatheter Closure of Atrial Septal Defects

Carsten Rickers, MD; Michael Jerosch-Herold, PhD; Xudong Hu, MD; Naveen Murthy, MD; Xiaoen Wang, MD; Huafu Kong, MD; Ravi Teja Seethamraju, PhD; Jochen Weil, MD; Norbert M. Wilke, MD

Background—Recent developments in cardiac MRI have extended the potential spectrum of diagnostic and interventional applications. The purpose of this study was to test the ability of MRI to perform transcatheter closures of secundum type atrial septal defects (ASD) and to assess ASD size and changes in right cardiac chamber volumes in the same investigation.

Methods and Results—In 7 domestic swine (body weight, 38±13 kg), an ASD (Q_p:Q_s=1.7±0.2) was created percutaneously by balloon dilation of the fossa ovalis. The ASD was imaged and sized by both conventional radiography and MRI. High-resolution MRI of the ASD diameters correlated well with postmortem examination (r=0.97). Under real-time MR fluoroscopy, the introducer sheath was tracked toward the left atrium with the use of novel miniature MR guide wires. The defect was then closed with an Amplatzer Septal Occluder. In all animals, it was possible to track and interactively control the position of the guide wire within the vessels and the heart, including the successful deployment of the Amplatzer Septal Occluder. Right atrial and ventricular volumes were calculated before and after the intervention by using cine-MRI. Both volumes were found to be significantly reduced after ASD closure (P<0.005).

Conclusions—These in vivo studies demonstrate that catheter tracking and ASD device closure can be performed under real-time MRI guidance with the use of intravascular antenna guide wires. High-resolution imaging allows accurate determination of ASD size before the intervention, and immediate treatment effects such as changes in right cardiac volumes can also be measured. **(*Circulation*. 2003;107:132-138.)**

Key Words: pediatrics ■ heart defects, congenital ■ magnetic resonance imaging

As ultrafast MRI technology improves and becomes more readily available, applications for catheter interventions in congenital heart disease could provide several practical advantages over current imaging modalities.[1–3] These advantages include interactive 3D steering of the imaging plane, excellent soft tissue contrast, and elimination or reduction of iodinated contrast agents and ionizing radiation. Additionally, high-resolution anatomic and functional imaging can be performed in the same study.[4,5] However, the capability of MRI for percutaneous device closure of intracardiac shunts has not yet been demonstrated. In the past 30 years, numerous devices have undergone investigation for percutaneous atrial septal defect (ASD) closure.[6,7] To perform MR-guided interventions, the ideal device should contain no ferromagnetic components, whereas its MR appearance should be different from myocardial tissue and blood.[8] The Amplatzer Septal Occluder (ASO, AGA Medical Corporation, Golden Valley, Minn) consists of a nitinol wire mesh that produces minimal artifacts and provides good tissue differentiation.[9]

This device is visible on MR images without causing a signal void in its proximity that would hamper interventional procedures. Transcatheter closure of secundum ASD under fluoroscopy with the use of retrievable devices has become a standard procedure in most pediatric cardiology centers and is considered to be a relatively straightforward procedure.[6,7,10]

Therefore, the purpose of this study was to explore the ability of MRI to (1) interactively control catheter tracking and targeting of the ASD with the use of recently developed intravascular antenna guide wires; (2) determine ASD size by high-resolution MRI, and compare it with balloon sizing by using radiographic fluoroscopy and postmortem examination; (3) perform ASD device closure under real-time and high-resolution MRI with the use of the ASO; and (4) measure outcome results from the intervention such as changes in right cardiac volumes.

Methods

Animal Preparation

Seven healthy swine from a University of Minnesota-owned pig farm (Minneapolis, Minn) were studied, and all animals were treated according to the "Guide for the Care and Use of Laboratory Animals" (NIH publication No. 80-23, revised 1985). A swine model

Received June 10, 2002; revision received September 8, 2002; accepted September 9, 2002.

From the University of Minnesota, Department of Radiology, Minneapolis, Minn (M.J.-H., X.H., N.M., X.W., H.K., R.T.S., N.M.W.); and University Hospital Hamburg-Eppendorf, Pediatric Cardiology, Germany (C.R., J.W.).

Correspondence to Norbert Wilke, MD, University of Florida, Cardiovascular MR and CT, Health Science Center, 655 West Eighth St, Jacksonville, FL 32209-6511. E-mail wilke@jax.ufl.edu

Circulation **is available at http://www.circulationaha.org** **DOI: 10.1161/01.CIR.0000039343.95540.CF**

Hemodynamic and Study Details

No.	Weight, kg	Pulmonary-to-Systemic Flow Ratio	Heart Rate,* bpm	Left Ventricular Pressure,* mm Hg	Device Size	Transseptal Puncture	Retrieval After Placement	Complications
1	32	1.7	95±23	85±12	12	No	No	. . .
2	67	1.5	75±11	102±18	12	No	No	Intermittent ventricular tachycardia
3	34	1.9	120±14	83±14	14	No	No	Rupture of left femoral vein
4	40	1.6	86±13	91±10	12	Yes	No	. . .
5	35	2.0	110±10	94±9	14	Yes	No	. . .
6	29	Not done	92±17	84±16	14	Yes	Yes	. . .
7	29	Not done	94±15	87±9	14	No	Yes	. . .

*Mean±SD.

was chosen because of the well-developed fossa ovalis and our institution's experience with this model for the development of ASD devices.[9] Preanesthesia was administered in the form of intramuscular Telazol/xylazine (1 mL/23 to 46 kg). After intubation, anesthesia was continued with 2% isoflurane and 98% oxygen. If a patent foramen ovale was not present, transseptal puncture was performed. An artificial ASD was created by dilating the fossa ovalis with a 12- or 14-mm balloon catheter (Impact, Braun Medical Inc), using conventional radiographic fluoroscopy. Blood gas measurements were obtained from the left atrium, main pulmonary artery, and superior vena cava to calculate the pulmonary-to-systemic flow ratio (Q_p:Q_s). ASD balloon sizing was then performed with an Amplatzer sizing balloon as described elsewhere.[11,12] After the study, the animals were observed for 12 hours in a postoperative care unit.

ASD Closure Device

The Amplatzer Septal Occluder is a double-disk device that is constructed from 0.004- to 0.008-inch nitinol wire without any ferromagnetic components. Further technical device details have been described elsewhere.[9]

MR ASD Sizing and Functional Imaging

The MRI studies were performed in a dedicated short-bore (160 cm length) cardiac MRI scanner (Sonata, Siemens Medical Systems) operating at a 1.5-T field strength. MR gradient-echo cine and spin-echo anatomic imaging were applied before and after the intervention to rule out any vascular or cardiac injury. The cine-images covered the entire cardiac cycle with ≈15 heart phases. The phase-encoding steps per k-space segment were adjusted to match the temporal resolution with the heart rate (TR per k-space segment/TE/flip angle=25 to 50 ms/4.8 ms/20°). Cardiac images of 6-mm-thick slices were acquired in both the long- and short-axis planes of the heart. To assess changes in right cardiac chamber volumes before and after ASD closure, right atrial and ventricular volumes and function were calculated from the short-axis cine-slices by using a cardiac image analysis package (Argus, Siemens Medical Systems). For better visualization of the atrial anatomy and the shunt, a fast T1-weighted gradient-echo sequence was used for MR angiography after a bolus administration of 10 mL of gadolinium-gadopentetate dimeglumine (Magnevist, Berlex).[12] The size of the defect was determined by using orthogonal short- and long-axis single-shot and cine-images. These measurements were repeated for the same slice position with an antenna guide wire (Surgi-Vision, Inc) crossing the ASD, which allows for a smaller field-of-view (FOV) without causing aliasing artifacts, and with the conventional external phase array coils turned off.[4,13,14] These measurements were compared with each other and with conventional balloon sizing and postmortem examination.

MRI-Guided Catheter Tracking and Intervention

Real-time images were acquired by interactive control of the image plane position with a 3D steering computer device ("Spacemouse") interfaced to the MR system. This 3D steering device is similar to a computer mouse but with the option of controlling positioning of the image slice in a third dimension by pulling or pushing a jog dial. Thus it was possible to follow a path to steer the catheter wire into vascular branches. Images appeared with a 0.5-second delay on an in-room display that provided continuous feedback. For guide wire positioning and high-resolution intravascular imaging, dedicated receive-only antenna guide wires were used.[14,15] The body coil was used for excitation of the signal in the user defined tomographic slice. Tissue and blood in the immediate vicinity of the guide wire antenna gave rise to relatively high signal intensity. Therefore, a thick slice could be used for real-time imaging to track the guide wire position within the slab.[16] Real-time MRI was performed with a steady-state free precession (SSFP) pulse sequence ("true FISP"; TR=1.4 ms, TE=1.15 ms, flip angle=40°, 50 to 60 phase-encodings, 128×128 image matrix, 7 to 15 frames per second, 1400 Hz/pixel, 35-mm slice thickness). We have found that SSFP imaging techniques as used in this study for real-time imaging provide a large signal-to-noise ratio gain over other gradient-echo techniques. Echo planar imaging was not used in this study because of its known susceptibility to flow-related artifacts.[17] With the real-time pulse sequence running under interactive user control and an MR image refresh rate of 5 images per second, a delivery sheath (AGA Medical) was tracked toward the left atrium. The ASO was attached to a custom-designed nitinol delivery cable (Kurt Amplatz, MD) and loaded into the delivery sheath. The ASO was then advanced under real-time MRI guidance to the tip of the sheath. Deployment of the ASO was monitored by passive tracking and interactively controlled by high-resolution real-time imaging. The left atrial button was released into the left atrium and pulled toward the atrial septum. The right disk was deployed by withdrawing the delivery sheath and the device was then disconnected from the cable. In 2 animals, the device was withdrawn into the delivery sheath after correct placement and redeployed for training purposes to simulate misplacement. The total duration for catheter tracking and ASO deployment was 20 minutes after 2 pilot studies.

High-Resolution Imaging

ASD sizing and proper positioning of the ASO before detachment was verified by high-resolution SSFP imaging (TR/TE 2.3/1.8 ms; flip angle 60°; 256 read-out points×100 phase encodings; 260 mm FOV; bandwith 900 Hz/pixel). Additional fast spin-echo imaging was applied to assess the exact anatomical position of the device (T2 TSE; TE 20 ms, TR 2352 ms, matrix 512×512, FOV 8.4×8.6 cm). The external receive-only coils were turned off during high-resolution anatomic imaging, providing us with an in-plane resolution of ≤1 mm. The signal-to-noise ratio could also be maintained at an acceptable level (>10:1) for a distance up to 8 cm from the intravascular antenna.[13,14]

Results

Dilation of the Fossa Ovalis and ASD Sizing

Percutaneous dilation of the fossa ovalis was possible without major complications in all 7 animals. Hemodynamic data and animal details are listed in the Table. ASD diameters in

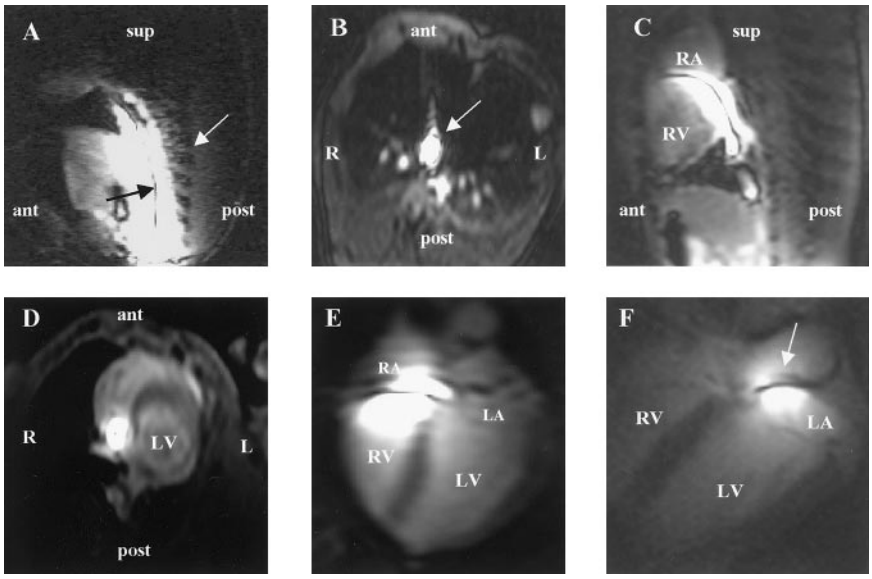

Figure 1. Guide wire tracking with a loopless miniature antenna wire. With the conventional external phased-array coils turned off, the short-range receiver profile makes the vicinity of the wire visible (white arrow, spine). In the initial frames (A, sagittal; B, coronal view) the antenna wire (black arrow) is advanced in the vena cava by using real-time MR fluoroscopy. The wire is advanced into the right atrium (C, sagittal; D, coronal view) and crosses the atrial septum (E) through the ASD. In the final frame (F), the wire (white arrow) is in the left atrium. Ant indicates anterior; post, posterior; sup, superior; L, left; and R, right.

millimeters obtained by using the Amplatzer sizing balloon with radiographic fluoroscopy correlated well with the unstretched postmortem examination ($y=0.94x+0.79$, $r=0.95$).

Catheter Tracking and MRI-Guided Intervention

MR fluoroscopy with the use of a fast gradient-echo sequence with SSFP can be performed at a sufficiently high frame rate to steer the antenna guide wire in the vena cava and the heart (Figure 1). The images were updated on the liquid crystal in-room display with a delay of <1 second, and the spatial in-plane resolution was high enough to see the catheter. With interactive control of the slice position, it was possible to continuously verify the anatomic position of the guide wire and the ASO (Figures 1 through 3).

High-Resolution Imaging

ASD sizes could be successfully determined from gradient-echo cine- and spin-echo imaging with an antenna guide wire positioned across the defect and turning the conventional external phase array coils off. This allowed for a reduction of the FOV (Figures 2 and 4). MR measurements with the antenna guide wire showed an excellent correlation of the maximal ASD diameter to postmortem examination ($y=1.02x-0.32$, $r=0.97$) in contrast to MR measurements obtained with the conventional external phase array coils alone ($y=0.91x+2.87$, $r=0.52$) (Figure 5).

Fast spin-echo and fast-gradient–echo high-resolution imaging after implantation showed successful closure of the ASD, with no cardiac or valvular damage. Both disks could be evaluated by using different slice positions (Figure 4, A through C). In some cases, the ASO caused a so-called ghosting artifact in the region of interest (Figure 4A). By swapping the phase-encoding direction, the direction of the artifacts was also swapped, allowing a clear visualization of the region of interest. A qualitative, visual comparison to other imaging modalities that are currently being used for percutaneous device closures of ASDs, such as echocardiography (Figure 4D) and fluoroscopy (Figure 4E), suggests that high-resolution MRI in conjunction with real-time MRI provides high image quality and visual feedback.

Assessment of Right Cardiac Volumes and Function

Measurements of right atrial and ventricular volumes obtained from gradient-echo cine-MRI before and 60 to 80 minutes after ASD closure is shown in Figure 6. Both right atrial (RA) and right ventricular (RV) volumes decreased significantly after the intervention (RA 26±7 mL versus 22±6 mL, $P<0.0046$; RV 37±10 mL versus 34±9 mL, $P<0.005$; 2-tailed, paired t test).

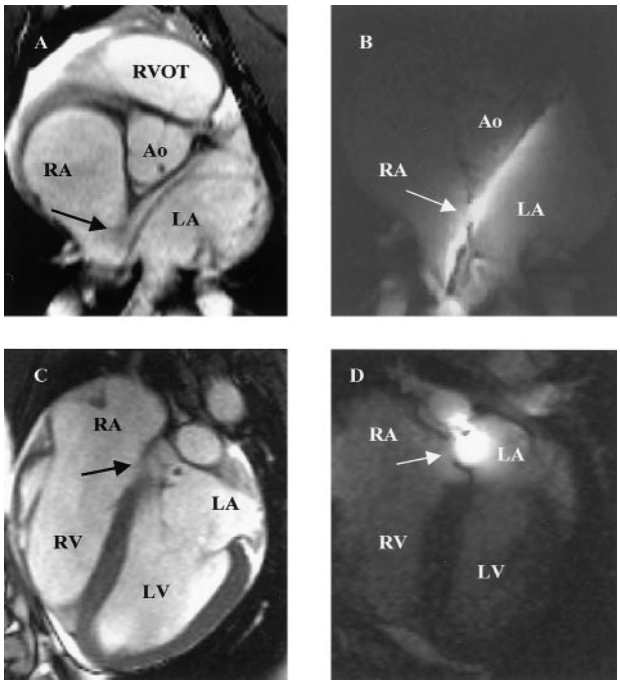

Figure 2. High-resolution images for assessment of guide wire position and ASD size. Images of anatomic short-axis (A, B) and long-axis (C, D) views. The guide wire is positioned across the ASD (arrows). Comparison of images with the conventional external phased-array coils turned on (A, C) versus images obtained with the guide wire antenna turned on alone (B, D).

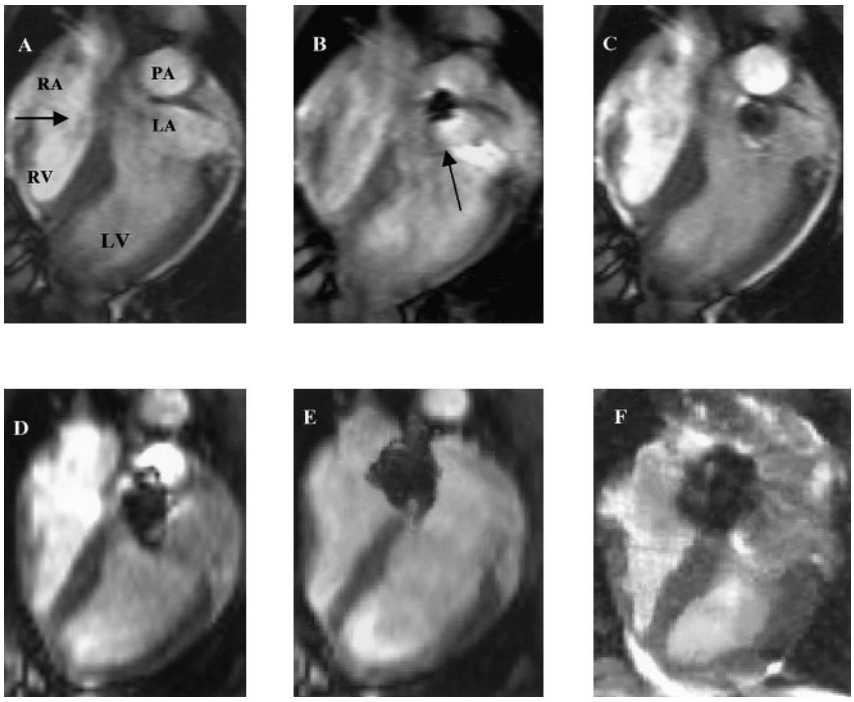

Figure 3. Series of long-axis 4-chamber snapshots with the use of "true FISP" real-time imaging sequence during placement of the ASO. For real-time imaging, the spatial resolution was reduced to increase the temporal resolution up 8 frames per second. Frame A shows the anatomy before implantation. Frame B shows the tip of the introducer sheath (black arrow) in the left atrium. Black artifact results from the nitinol device in the tip of the sheath. Partial deployment of the left atrial disk (C). Complete deployment of the left atrial disk (D). Right atrial disk becomes visible after partial deployment (E). Occluder appears in the area of the fossa ovalis after disconnection from the delivery cable (F).

Pathology

The findings of high-resolution imaging were compared with postmortem examination (Figure 7). In all 7 animals, gross anatomy showed no cardiac or vascular injury. In the 5 animals in which the device was disconnected from the delivery cable, the ASO was covering the region of the fossa ovalis without compromising the ostia of the left pulmonary veins, the coronary sinus, or the tricuspid and mitral valves. We found thrombus inside the device in all cases but no surface thrombus, as expected.

Discussion

The latest generation of interactive cardiac MR scanners with ultrafast MRI techniques have made it possible to perform real-time imaging with interactive control of the tomographic imaging plane.[1,2,15,17] In this in vivo study, we demonstrated

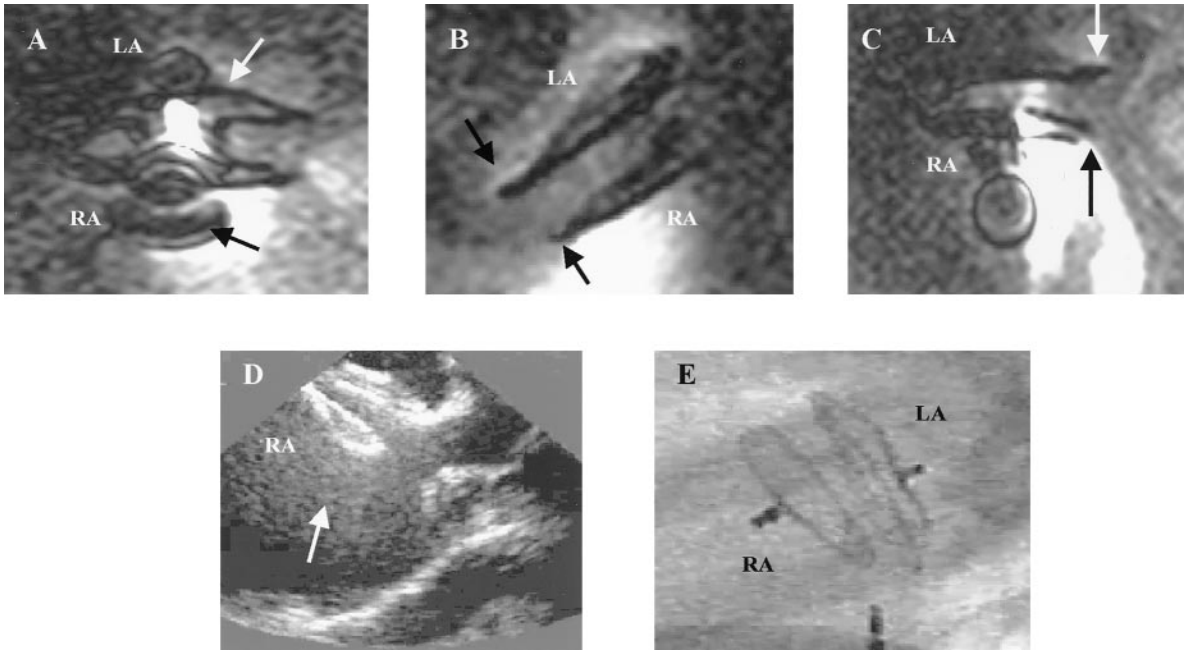

Figure 4. High-resolution imaging for evaluation of correct device position (A through C). Nitinol device (white arrow) with small ghosting artifact (black arrow). Typical sandwich-like position of the device with both disks on either side of the posterior septum (arrows) (B). Evaluation of the anterior rim shows some splaying of the device at the aortic root (arrows) (C). Comparison with other imaging modalities: transesophageal echo (D) and radiographic fluoroscopy (E).

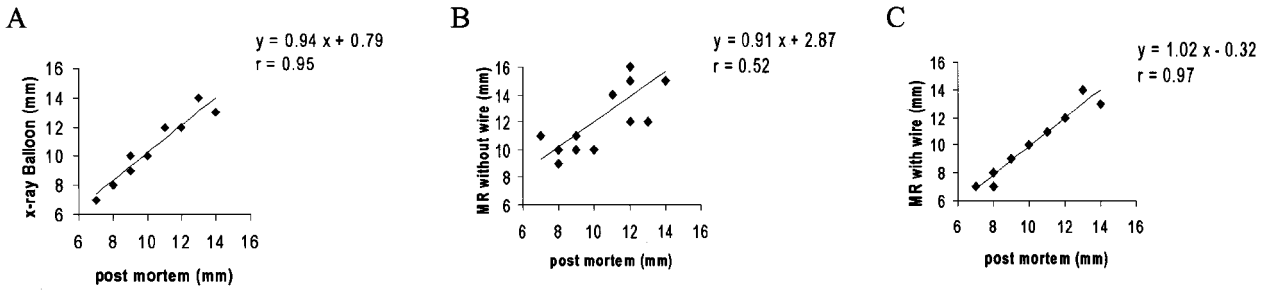

Figure 5. Comparison of different sizing methods for determination of maximal and minimal ASD diameter. Balloon sizing (A) and high-resolution MRI with antenna guide wires (C) correlated well with postmortem examination. MRI sizing without antenna wire did not correlate well with postmortem examination (B).

for the first time the ability to perform transcatheter ASD closures under MRI guidance. Furthermore, it was possible to size the ASD and monitor changes in cardiac volumes and function during the same MR investigation.

Catheter Tracking and Device Placement

Guide wire and device tracking is a prerequisite for MRI-guided cardiac interventions. Unlike MRI-guided interventions in static organs such as the brain,[18] interventions in the heart pose a difficult challenge because of its constant motion. MRI artifacts from cardiac and diaphragmatic motion can only be overcome by rapid imaging, which should provide high spatial and temporal resolution simultaneously.[13] Although both active and passive tracking methods have been proposed,[4,14–16] active tracking with miniature radiofrequency antennas mounted on the tip of a catheter wire appears to be the method of choice for performing ASD closures under MRI guidance.

We used a loopless miniature antenna guide wire for active tracking in the vena cava and the heart (Figure 1).[14,16] By using the aforementioned 3D steering device with real-time MRI imaging at a rate of 5 to 8 images per second, we were able to continuously verify the anatomic position of the guide wire and the ASO (Figures 1 and 3). In our experience, the use of "active guide wires" under MR fluoroscopy provided visual feedback to the operator as conventional radiographic fluoroscopy, albeit with a lower frame rate. This lower frame rate did not represent a limitation in this study. Real-time MRI does not require ECG gating and thus is not limited to fast heart rates. MR fluoroscopy was carried out for thick slabs (3 to 5 cm) to determine the in-plane position of the wire or the device and reduce the sensitivity to motion of the heart relative to the fixed slab position. The very high signal intensities from tissue and blood in close vicinity to the antenna resulted in a projection-type image (Figure 1). Once the device was in the intended position, it was possible to switch to imaging of thin slices within 5 seconds and ECG gate the image acquisition to completely freeze out cardiac motion (Figure 2 and 4). This allows passive MR tracking of the ASO deployment under real-time MRI (Figure 3). Passive tracking relies on magnetic susceptibility artifacts, or signal voids, generated by a device or catheter caused by inhomogeneities in the magnetic field.[15]

ASD Sizing

Visualization of shunt flow with gradient-echo cine and ASD sizing by spin-echo imaging have been described earlier.[19] Both techniques were found to be suboptimal for determination of ASD dimensions. Spin-echo imaging overestimates the defect due to "signal dropout" resulting from the thinning in the area of the fossa ovalis.[19] Gradient-echo cine-MRI may not be able to visualize shunt flow in all cases, in particular with low interatrial pressure gradients as they occur with small ASDs or patent foramen ovale. To improve the spatial resolution ($<$1 mm), we used antenna guide wires that crossed the ASD (Figure 2), allowing for a very small FOV (eg, 5$\times$5 cm).[4,5] We found an excellent correlation between this method of ASD sizing and postmortem sizing, compared

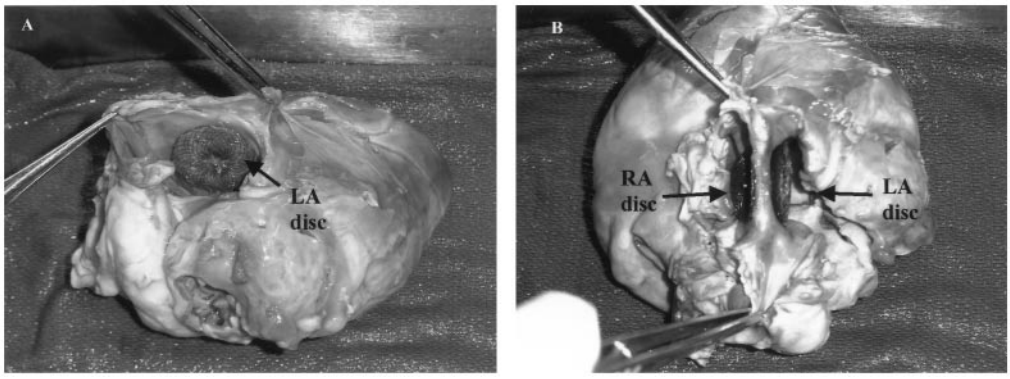

Figure 6. Postmortem examination of the heart confirms correct device position in the area of the fossa ovalis (A), with both disks on either side of the septum (B).

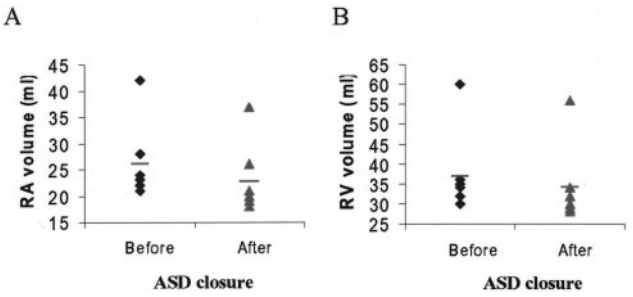

Figure 7. Significant reduction in right cardiac chamber volumes could be observed for both the right atrium (A) and the right ventricle (B) after ASD closure ($P<0.005$). Bars indicate mean values.

with conventional gradient-echo cine-MRI without antenna guide wires (Figure 5).

Assessment of Cardiac Volumes and Function

Cardiac-gated cine-MRI has been found to provide a reliable means to assess atrial and ventricular volumes and function.[20] Applying this protocol before and after the intervention resulted in an additional 15 to 20 minutes scan time. We found a decrease in RA and RV volumes after ASD closure (Figure 6). These findings were consistent with echocardiographic measurements of a decrease in RA area and RV volumes within 24 hours after ASD closure.[21]

Clinical Implications

Radiographic imaging in conjunction with transesophageal echocardiography is the current modality of choice for ASD sizing, closure, and other cardiovascular catheter interventions for all age groups.[6,7,10] 2D and 3D MRI provides excellent soft tissue contrast and avoids exposure to ionizing radiation. Ionizing radiation becomes an issue in more complex, lengthy procedures as opposed to relatively straightforward ASD closures.[22] However, to appreciate this potential MRI advantage, studies must be performed in simpler, shorter procedures before more complex, lengthy procedures are tried, such as closure of ventricular septal defects. MRI also uses a noniodinated contrast agent, gadolinium, that has no reported adverse effects.[23] Furthermore, MRI allows for concurrent ASD sizing and right cardiac volume measurements.

To conduct clinical studies in humans and especially in pediatric patients, any remaining safety concerns have to be addressed conclusively. Magnetic fields oscillating at radiofrequencies, as used for MRI, may induce significant heating in long metallic wires. In particular, if standing waves form along the conductive catheter wires in the body, they can cause thermal injury.[24,25] The guide wires that were used in this study were connected to a radiofrequency decoupling/tuning box that limited the energy transferred by the radiofrequency pulses.[4,14] Heating experiments in our laboratory performed with a gel phantom and applying a fast spin-echo and an SSFP sequence showed no adverse temperature changes (>0.3°C) near the wires (specifically at the tips) or the ASO as measured by fiberoptic sensors. Testing with different guide wire configurations and placement at off-center positions within the magnetic field did not alter the findings.

Practicality and ease of use is another important aspect in performing complex cardiovascular interventions. Interventional MRI-guided percutaneous procedures require direct access to the groin and neck for manipulation of catheters and devices. In our studies in a short-bore magnet, we were able to manipulate the catheters from the groin. Open-sided MR systems would be ideal but are limited by a low static magnetic field strength that reduces the signal-to-noise ratio, making the resultant images unacceptable for cardiac interventions.[1,18] Widespread application of interventional MRI is hampered by the limited commercial availability of nonmagnetic guide wires, delivery cables, monitoring equipment, and retrieval systems in the event of device embolization

Conclusions

These experiments demonstrated that a secundum ASD can be closed under MR guidance by using new fluoroscopic MR technology in conjunction with active guide wire tracking. High-resolution MRI allowed correct assessment of ASD size and ASO position. Cine-MRI allowed assessment of changes in right cardiac chamber volume after ASD closure. In the future, this powerful diagnostic tool may evolve into an alternative or a complementary interventional tool for complex cardiac procedures.

Acknowledgments

Carsten Rickers, MD, was supported in part by a grant from the German Research Society (DFG No. RI 1040/1-1) and by NIH RO1-HL6539. We thank Kurt Amplatz, MD, and Franck Gougeon from AGA Medical for their advice and for providing us with the Amplatzer Septal Occluder and customized nitinol delivery cables. We also thank Ingmar Viohl, PhD, from Surgi-Vision, Inc, for his help in conducting the temperature measurements.

References

1. Lardo AC. Real-time MRI: diagnostic and interventional applications. *Pediatr Cardiol*. 2000;21:80–98.
2. Kerr AB, Pauly JM, Hu BS, et al. Real-time interactive MRI on a conventional scanner. *Magn Reson Med*. 1997;38:355–367.
3. Lardo AC. Real-time MRI applications: in vitro demonstration of the potential of MRI for guiding, monitoring, and evaluating endovascular interventions. *J Magn Reson Imaging*. 1999;8:245–250.
4. Atalar E, Bottomley PA, Ocali O, et al. High resolution intravascular MRI and MRS by using a catheter receiver coil. *Magn Res Med*. 1996;36:596–605.
5. Lardo AC, McVeigh ER, Jumrussirikul P, et al. Visualization and temporal/spatial characterization of cardiac radiofrequency ablation lesions using magnetic resonance imaging. *Circulation*. 2000;102:698–705.
6. Austin EH. Editorial: transcatheter closure of atrial septal defects (review). *J Thorac Cardiovasc Surg*. 2000;120:1032–1033.
7. Syamasundar RP, Sideris EB. Transcatheter closure of atrial septal defects. *Heart*. 1999;82:644.
8. Strouse PJ, Beekman RH. Magnetic deflection forces from atrial septal defect and patent ductus arteriosus-occluding devices, stents, and coils used in pediatric-aged patients. *Am J Cardiol*. 1996;78:490–491.
9. Sharafuddin MJ, Gu X, Titus JL, et al. Transvenous closure of secundum atrial septal defects: preliminary results with a new self-expanding nitinol prosthesis in a swine model. *Circulation*. 1997;95:2162–2168.
10. Zahn EM, Wilson N, Cutright W, et al. Development and testing of the Helex septal occluder, a new expanded polytetrafluoroethylene ASD occlusion system. *Circulation*. 2001;7:104:711–716.
11. Gu X, Han YM, Berry J, et al. A new technique for sizing of atrial septal defects. *Cathet Cardiovasc Interv*. 1999;46:51–57.

12. Manning WJ, Atkinson DJ, Parker JA, et al. Assessment of intracardiac shunts with gadolinium-enhanced ultrafast MR imaging. *Radiology*. 1992;184:357–361.
13. Hu X, Parrish T. Reduction of field of view for dynamic imaging. *Magn Reson Med*. 1996;31:691–694.
14. Ocali O, Atalar E. Intravascular magnetic resonance imaging using a loopless catheter antenna. *Magn Reson Med*. 1997;37:112–118.
15. Bakker CJ, Hoogeveen RM, Weber Jet al. Visualization of dedicated catheters using fast scanning techniques with potential for MR-guided vascular interventions. *Magn Reson Med*. 1996;36:816–820.
16. Ladd ME, Erhart P, Debatin JF, et al. Guidewire antennas for MR fluoroscopy. *Magn Reson Med* . 1997;37:891–897.
17. Reeder SB, Atalar E, Faranesh AZ, et al. Multi-echo segmented k-space imaging: an optimized hybrid sequence for ultrafast cardiac imaging. *Magn Reson Med*. 1999;41:375–385.
18. Kollias SS, Bernays R, Manugg RA, et al. Target definition and trajectory optimization for interactive MR-guided biopsies of brain tumors in an open configuration MRI system. *J Magn Reson Imaging*. 1998;8: 143–159.
19. Holmvang G, Palacios IF, Vlahakes GJ, et al. Imaging and sizing of atrial septal defects by magnetic resonance. *Circulation*. 1995;92:3473–3480.
20. Poutanen T, Ikonen A, Vainio P, et al. Left atrial volume assessed by transthoracic three dimensional echocardiography and magnetic resonance imaging: dynamic changes during the heart cycle in children. *Heart*. 2000;83:537–542.
21. Kort HW, Balzer DT, Johnson MC. Resolution of right heart enlargement after closure of secundum atrial septal defect with transcatheter technique. *J Am Coll Cardiol*. 2001;38:1528–1532.
22. Shim D, Kimball TR, Michelfelder EC, et al. Exposure to ionizing radiation in children undergoing Amplatzer device placement to close atrial septal defects. *Cathet Cardiovasc Interv*. 2000;51:451–454.
23. Nelson KL, Gifford LM, Lauber-Huber C, et al. Clinical safety of gadopentetate dimeglumine. *Radiology*. 1995;196:439–443.
24. Nitz W, Oppelt A. On the heating of linear conductive structures as guide wires and catheters in interventional MRI. *J Magn Reson Imaging*. 2001; 13:105–114.
25. Budinger TF. Nuclear magnetic resonance in vitro studies: known thresholds for health effects. *J Comput Assist Tomogr*. 1981;5:800–811.